Article

Femtosecond Laser-Written Small-Period Long-Period Fiber Grating for an L-Band Normal Dispersion Mode-Locked Fiber Laser

Qianying Li, Peiyun Cheng, Rong Zhao and Xuewen Shu *

Wuhan National Laboratory for Optoelectronics & School of Optical and Electronic Information, Huazhong University of Science and Technology, Wuhan 430074, China; qianyli@hust.edu.cn (Q.L.); pycheng@hust.edu.cn (P.C.); zhaorong@hust.edu.cn (R.Z.)
* Correspondence: xshu@hust.edu.cn

Abstract: We utilize a femtosecond laser-inscribed small-period long-period fiber grating (SP-LPFG) to induce a nonlinear polarization rotation (NPR) effect for mode-locking pulses in a normal dispersion erbium-doped fiber laser (EDFL). The SP-LPFG has a length of 2.5 mm and a period of 25 μm. At wavelengths of 1556 nm and 1561 nm, it exhibits polarization-dependent loss (PDL) values of 20 dB and 14.5 dB, respectively, sufficient to trigger the NPR mechanism. With the pump power increased to 500 mW, the laser achieves normal dispersion mode-locked pulses centered at 1575 nm in the L-band, with a 3 dB bandwidth of 1.35 nm and a pulse width of 1.61 ps. The radio frequency (RF) spectrum reveals an signal-to-noise ratio (SNR) of up to 63.6 dB, demonstrating the excellent stability of the laser operation. This SP-LPFG holds promising applications, paving the way for efficient, compact, and stable normal dispersion ultrafast fiber lasers.

Keywords: fiber laser; mode-locked pulses; nonlinear polarization rotation; polarization-dependent loss

1. Introduction

In recent years, there has been significant interest among researchers in the potential applications of ultrafast fiber lasers operating in the L-band (1565–1625 nm) in fields such as spectral analysis, biomedical sciences, optical sensing, and telecommunications [1,2]. As the demand for optical communication systems continues to grow, L-band lasers have garnered more attention due to their superior gain flatness compared to that of C-band lasers, as well as less silica fiber loss in this spectral region [3,4].

Passive mode-locked fiber lasers can be achieved using various saturable absorbers (SAs). Among them, equivalent SAs exploit the nonlinear effects of different structured optical devices, primarily including NPRs [5–8], nonlinear optical loop mirrors (NOLMs) [9,10], nonlinear amplifying loop mirrors (NALMs) [11,12], nonlinear multimode interference (NLMMI) [13–15], and so on. NPR technology has become a conventional method for achieving ultrashort pulses in fiber laser systems, leading to narrower pulse widths and higher pulse energies [16,17]. NPR mode locking is typically achieved using polarization-dependent optical isolators and polarization controllers (PCs) [18]. However, these devices suffer from considerable insertion losses (ILs) and poor compactness, which hinder the development of integrated fiber lasers. Therefore, NPR mode locking based on various novel fiber structures has also attracted considerable attention and extensive research. In 2010, Mou et al. first utilized the polarization properties of a 45° tilted grating to successfully construct an erbium-doped mode-locked fiber laser (MLFL) [19]. In 2016, Du et al. proposed a unique chiral grating fiber polarizer and achieved mode-locking pulses using NPR technology [20]. In 2022, Alamgir et al. developed a tapered sulfur compound fiber, generating tunable soliton pulses using NPR technology [21]. Inspired by these studies, we intend to utilize advanced fiber SAs to achieve mode-locking pulses in fiber lasers.

Fiber gratings have rapidly developed as fiber devices in recent years, forming periodic refractive index changes in the fiber core using specific methods. They exhibit

characteristics, such as low loss, a wide bandwidth, and immunity to electromagnetic interference [22,23]. Long-period fiber gratings (LPFGs), as all-fiber mode couplers, possess high refractive index sensitivity and allow for mode coupling control by adjusting the grating parameters. They have been widely applied in fiber sensing and fiber communications [24–27]. The SP-LPFG is a type of long-period grating with a smaller period, typically in the range of tens of micrometers, which exhibits significant polarization-dependent properties due to mode coupling with higher-order cladding modes [28]. Some researchers have successfully demonstrated pulsed fiber lasers based on tilted fiber Bragg gratings (TFBGs) [29,30]. TFBGs enable mode-locking mechanisms through the coupling between core modes and cladding or radiation modes, facilitated by their polarization properties. Similarly, SP-LPFGs exhibit characteristics similar to TFBGs, where the guided modes can couple with higher-order cladding modes, demonstrating significant vector behaviors that lead to strong polarization dependence. This polarization dependence in SP-LPFGs results in higher PDL at certain wavelengths. By adjusting the polarization state, significant control over optical loss is achieved, thereby regulating the input light intensity effectively. By optimizing the polarization controller to a suitable angle, high-energy portions of light pass through, while the low-energy portions are suppressed. This cyclic process repeats to ultimately form ultrashort pulses, representing the core principle of NPR technology. Compared to the other types of fiber-based mode-lockers, SP-LPFGs offer quicker processing and superior structural integration.

In this work, to our knowledge, we first utilized femtosecond laser-written SP-LPFGs as a mode locker for achieving mode-locked pulses in normal dispersion L-band fiber lasers. The SP-LPFG with a period of 25 μm and a length of 2.5 mm was inscribed on a single-mode fiber, exhibiting PDL values of up to 20 dB at 1556 nm and 14.5 dB at 1561 nm wavelengths. The integration of the SP-LPFG into a normal dispersion erbium-doped fiber laser resulted in mode-locked pulses centered at 1575 nm, with a 3 dB bandwidth of 1.35 nm and a pulse duration of 1.61 ps. The SP-LPFG provides a novel approach and solution for implementing normal dispersion mode-locked fiber lasers.

2. Fabrication and Characterization of the SP-LPFG

The SP-LPFG used in this research is directly inscribed onto standard single-mode fiber (SMF) using a femtosecond laser with the point-by-point method. The schematic diagram of the femtosecond laser-inscription system is shown in Figure 1a, operating at a wavelength of 520 nm, with a repetition rate of 200 kHz, and a pulse energy of 40.3 nJ. Prior to inscription, several drops of matching oil with a refractive index of 1.518 RIU are applied to the glass slide to ensure the accuracy and efficiency of the inscription process. During the experiment, the fiber is straightened and placed on the glass slide to ensure precise laser interaction. The laser beam is focused on the fiber by a 63× oil-immersion objective lens with a numerical aperture of 1.4. The length and period of the grating are adjusted via computer-controlled XYZ translation stages, while the laser-inscription process is monitored in real-time using a CCD camera. One end of the fiber is connected to a broadband source (BBS), while the other end is observed through an optical spectrum analyzer (OSA) to examine the transmission characteristics of the inscribed fiber grating. A schematic of the inscription process is depicted in the Figure 1b. A constant translation speed of 50 μm/s along the fiber axis is set to ensure the stability and continuity of the inscription process. Moreover, to optimize the performance of the SP-LPFG, we set the period to 25 μm and the length to 2.5 mm.

To investigate the influence of polarization states on the transmission spectrum intensity, a measurement system is constructed. The system comprises an amplified spontaneous emission (ASE) light source, a polarizer, a PC, and a spectrometer. In the experiment, the SP-LPFG is integrated into the setup, connected to an ASE source around the 1550 nm wavelength, and the polarization state of the system is adjusted using the PC. Simultaneously, the transmission spectra of the SP-LPFG under different polarization states are measured using the OSA. The transmission spectra of the SP-LPFG under polarization

states P1 and P2 are recorded in Figure 2a. Obviously, there is a significant difference in the intensities of transmission peaks. Therefore, the SP-LPFG exhibits high PDL characteristics around the 1550–1560 nm range. For an in-depth investigation of the PDL characteristics of SP-LPFG, a commercial VIAVI MAP-300 multi-application platform is employed to characterize the PDL values at different wavelengths. The wavelength scanning range is set between 1550 nm and 1600 nm, with a resolution of 3 pm. The characteristic curve of PDL variation with wavelength is shown in Figure 2b. At wavelengths of 1556 nm and 1561 nm, the PDL values reach as high as 20 dB and 14.5 dB, respectively, demonstrating the strong polarization dependence of the grating sufficient to induce the generation of NPR mode-locking effects.
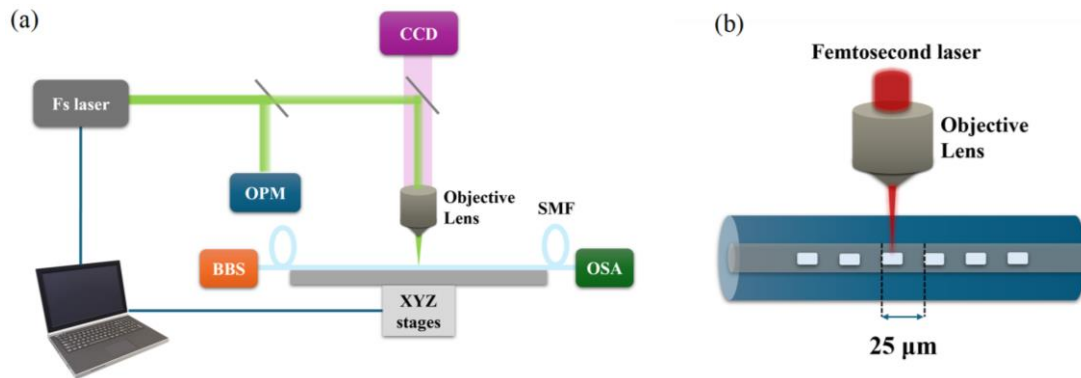

Figure 1. (**a**) A schematic diagram of the femtosecond laser inscription system. CCD: Charge-coupled Device; OPM: Optical Power Meter; BBS: broadband source; OSA: optical spectrum analyzer. (**b**) A schematic of the femtosecond laser-inscription process for the SP-LPFG.
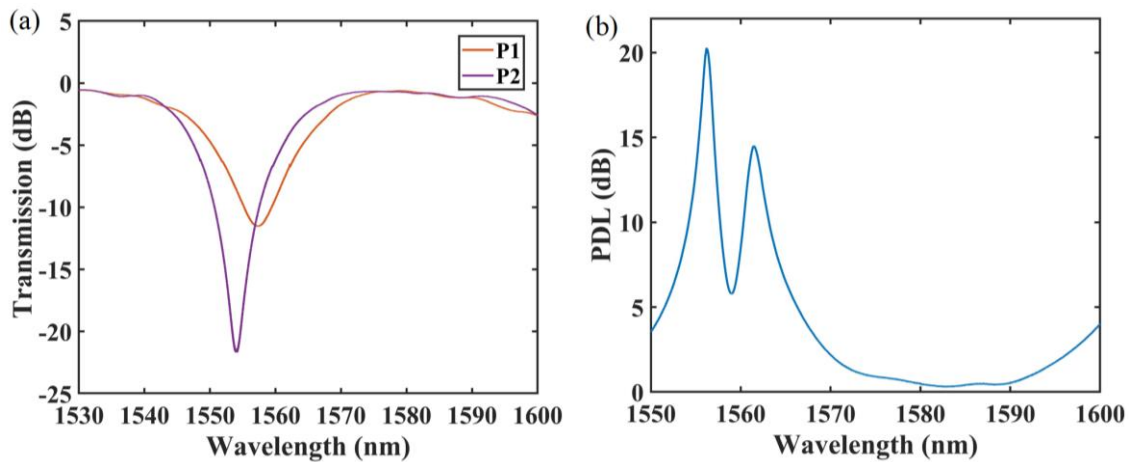

Figure 2. (**a**) The measured transmission spectra of the SP-LPFG from 1530 nm to 1600 nm range at different polarization states. (**b**) The measured PDL response of the SP-LPFG.

Typically, the PDL of SP-LPFGs is closely correlated with the parameters set during their fabrication process, including the period, length, and writing intensity. Setting the processing period and the length of gratings either too long or too short is detrimental to optimizing their transmission performance. Generally, increasing the laser writing intensity enhances the PDL of gratings, accompanied by an increase in insertion loss (IL). Improper parameter selection may result in a significant reduction in PDL, thereby adversely affecting the mode-locking stability of fiber lasers. Therefore, selecting appropriate processing parameters is crucial for obtaining a high-quality SP-LPFG mode locker.

3. Experimental Setup of the Fiber Laser

A schematic diagram of the constructed normal dispersion EDFL with the SP-LPFG is shown in Figure 3. The gain medium consists of a 2.4 m length erbium-doped fiber (Fibercore I-25 980/125), exhibiting a group velocity dispersion of −26 ps/nm/km at a wavelength of 1550 nm, pumped by a laser diode (LD) centered at 976 nm through a 980/1550 nm wavelength division multiplexer (WDM). A polarization-independent isolator (PI-ISO) is employed to ensure the unidirectional propagation of light within the laser cavity. A 7 m dispersion compensating fiber (DCF, YOFC G.652 C/250) is introduced into the fiber laser cavity, where its group velocity dispersion reaches −140.9 ps/nm/km at a wavelength of 1545 nm. The DCF effectively provides adequate normal dispersion to compensate for the intrinsic anomalous dispersion of single-mode fiber, allowing for the precise control of the dispersion value within the laser cavity. To achieve flexible polarization state adjustment and rapid mode locking, PCs are installed at both ends of the SP-LPFG. This allows for the precise adjustment of the polarization state to induce and maintain a stable mode-locking state within the laser cavity. The total length of the fiber laser cavity is approximately 45 m, with a dispersion value of 0.554 ps². The laser output is extracted through 10% port of a coupler, while the remaining 90% of the light is fed back into the cavity to sustain continuous laser oscillation. A second optical coupler (90:10) is used for simultaneously external connection to multiple devices for data measurement. The performance of the output laser is observed using an OSA (Yokogawa AQ6370) and a 500 MHz digital oscilloscope (Rigol-DS4052), with detection facilitated by a 5 GHz photodetector (Thorlabs-DET08CFC). RF spectrum analyzers (Rohde&Schwarz-FSH20) are used to analyze spectral characteristics, while an autocorrelator (APE-Pulse Check) is employed for the precise measurement of the pulse shape and width.
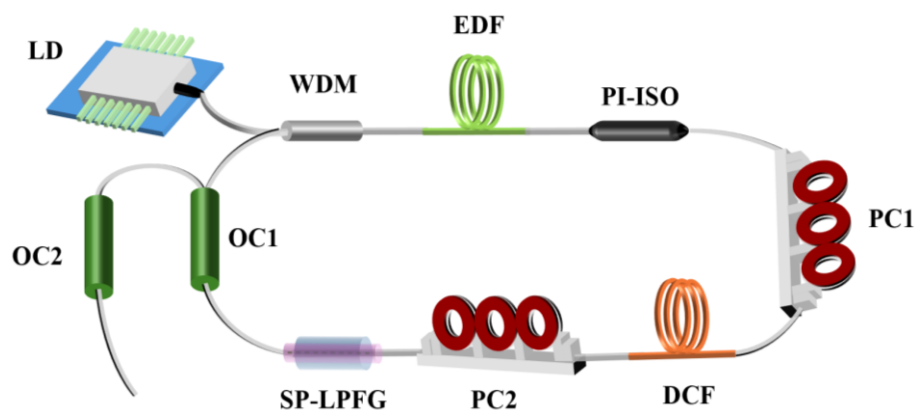

Figure 3. A schematic diagram of the normal dispersion mode-locked fiber laser based on the femtosecond laser-inscribed SP-LPFG.

4. Results and Discussion

Firstly, without integrating the SP-LPFG into the fiber laser, the attempts to induce mode-locking pulses by increasing the pump power and adjusting the angles of the polarization controllers did not yield any observable mode-locking phenomena. Subsequently, by inserting the SP-LPFG and adjusting the PCs, stable mode-locked pulses with a threshold power of 500 mW were successfully achieved in the normal dispersion regime. Due to the combined effects of bend loss in the fiber within PCs and insertion loss introduced by optical components, the mode-locking threshold did not reach the ideal minimum value. Figure 4a illustrates the evolution of the mode-locking spectrum as the pump power increases from 500 mW to 700 mW. The central wavelengths of the spectrum are about at 1575 nm, with a 3 dB bandwidth maintained around 1.35 nm. As the pump power gradually increases, the spectral intensity enhances, accompanied by a slight increase in spectral bandwidth. After that, temporal signals of the fiber laser are recorded, showing a stable pulse sequence, as depicted in Figure 4b. The measured pulse interval is 224 ns,

corresponding to the cavity length. Due to the resolution limit of the oscilloscope, the autocorrelation trace of the mode-locked pulses is measured using an autocorrelator, with a full width at half maximum (FWHM) of 2.49 ps, shown in Figure 4c, consistent with the theoretical sech² pulse shape. The actual pulse width is calculated to be 1.61 ps.
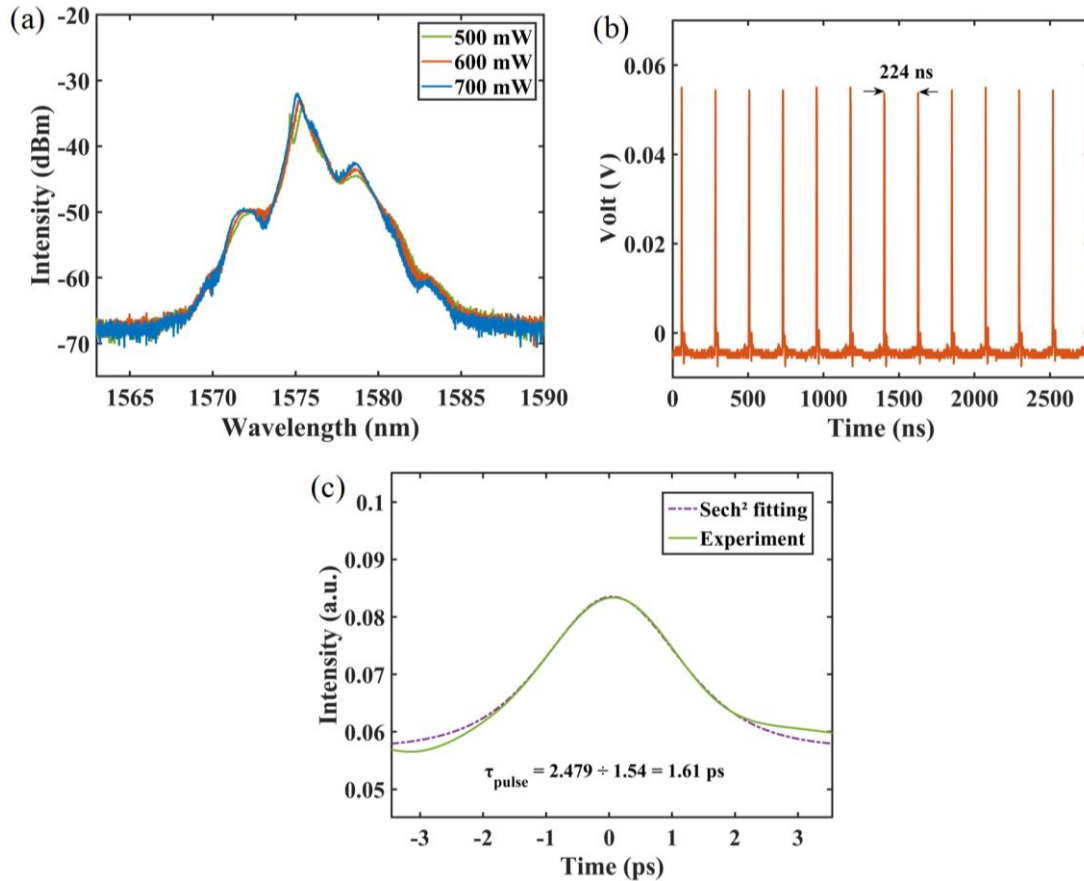

Figure 4. The performances of the mode-locked fiber laser in the normal dispersion using the SP-LPFG. (**a**) Optical spectrum; (**b**) pulse train; (**c**) autocorrelation trace with sech^2 fitting.

In addition, the RF spectrum is shown in Figure 5a, obtaining a spectrum with a span of 9 MHz and a resolution of 3 kHz. The SNR of the fundamental peak reaches up to 63.6 dB, demonstrating the excellent robustness and stability of the mode-locked pulses. Figure 5b presents the RF spectrum recorded over a wider frequency range, showing a stable overall attenuation trend. Moreover, continuous monitoring is conducted over a period of 4 h to record the optical spectral evolution of mode-locked pulses over time, further verifying their stability. For a more intuitive representation of this stability, a false-color graph of the spectrum was generated, as shown in Figure 5c. From the plot, it is evident that over the 4 h monitoring period, the spectrum maintains consistent mode-locking characteristics, without significant temporal variations or distortions.

To enhance the output performance of mode-locked fiber lasers, effective optimization measures can be implemented. An important way to optimize the performance of mode-locked fiber lasers is to reduce the IL of the SP-LPFG. Firstly, incorporating an aperture for beam filtering before femtosecond laser inscription enhances the precision and quality of grating structures, thereby optimizing its IL to a certain extent. Secondly, appropriately reducing the femtosecond writing power reduces the IL intensity, thereby minimizing its impact on the output of mode-locked fiber lasers. Moreover, shortening the length of the laser cavity is also an effective approach. During laser propagation within the cavity, the inherent properties of the fiber material, such as absorption and scattering, affect the process, leading to the attenuation of optical intensity. Increasing the length of the laser

cavity exacerbates this transmission loss. Therefore, the precise control of the laser cavity length not only maintains stable laser performance, but also reduces the transmission losses, thereby enhancing the output efficiency of the laser.
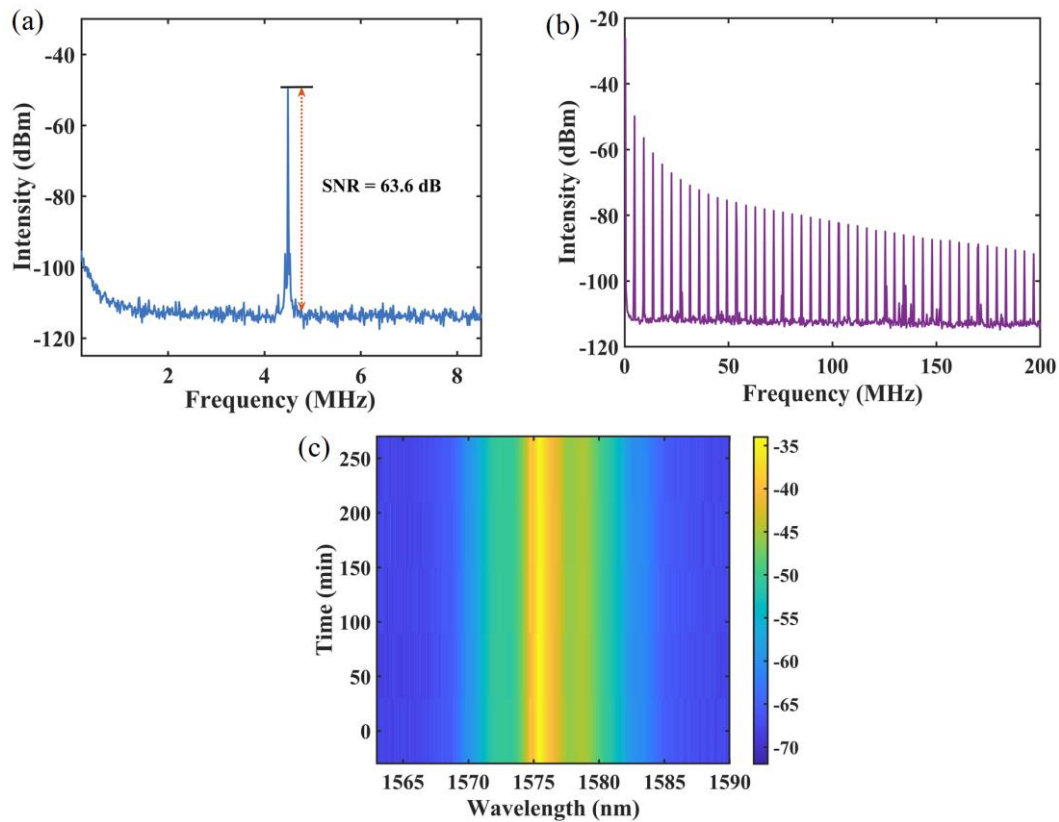

Figure 5. The frequency spectra and stability of the mode-locked fiber laser in normal dispersion based on the SP-LPFG. (**a**) the RF spectrum over a short span; (**b**) the RF spectrum over a short span; (**c**) the stability of the optical spectra.

The SP-LPFG mode locker not only provides an innovative solution for optimizing fiber laser mode locking, but also demonstrates promising applications in fiber sensing [31,32]. Through external intervention, the SP-LPFG enables the flexible adjustment of transmission spectral operating wavelengths. Therefore, based on its optical characteristics, SP-LPFGs have the potential to serve simultaneously as wavelength-tunable filters and mode lockers, offering possibilities for developing wavelength-tunable mode-locked fiber lasers.

5. Conclusions

In summary, we have demonstrated a stable, all-fiber, L-band, mode-locked fiber laser in normal dispersion using a femtosecond laser-inscribed SP-LPFG. This SP-LPFG has a period of 25 μm and a length of 2.5 mm. At the wavelengths of 1556 nm and 1561 nm, the PDL values reach 20 dB and 14.5 dB, respectively. With the pump power increased to 500 mW, the normal dispersion mode-locked optical spectrum is centered at 1575 nm, with a 3 dB bandwidth of 1.35 nm, and an actual pulse width of 1.61 ps. The RF spectrum exhibits an SNR of up to 63.6 dB, providing strong evidence of the high stability of the mode-locked pulses. As a novel mode locker, the SP-LPFG features a straightforward manufacturing process and great structural integration, suitable for developing compact, robust all-fiber ultrafast lasers, thus offering a promising avenue for the advancement of tunable mode-locked fiber lasers.

Data Availability Statement: Data underlying the results presented in this paper are not publicly available at this time, but may be obtained from the authors upon reasonable request.

Conflicts of Interest: The authors declare no conflicts of interest.

References

1. Marshall, J.; Stewart, G.; Whitenett, G. Design of a tunable L-band multi-wavelength laser system for application to gas spectroscopy. *Meas. Sci. Technol.* **2006**, *17*, 1023–1031. [CrossRef]
2. Cadroas, P.; Abdeladim, L.; Kotov, L.; Likhachev, M.; Lipatov, D.; Gaponov, D.; Hideur, A.; Tang, M.; Livet, J.; Supatto, W.; et al. All-fiber femtosecond laser providing 9 nJ, 50 MHz pulses at 1650 nm for three-photon microscopy. *J. Opt.* **2017**, *19*, 065506. [CrossRef]
3. Sun, Z.; Rozhin, A.G.; Wang, F.; Scardaci, V.; Milne, W.I.; White, I.H.; Hennrich, F.; Ferrari, A.C. L-band ultrafast fiber laser mode locked by carbon nanotubes. *Appl. Phys. Lett.* **2008**, *93*, 061114. [CrossRef]
4. Agrawal, G.P. *Lightwave Technology: Telecommunication Systems*; John Wiley & Sons: Hoboken, NJ, USA, 2005.
5. Huang, Z.; Huang, Q.; Theodosiou, A.; Cheng, X.; Zou, C.; Dai, L.; Kalli, K.; Mou, C. All-fiber passively mode-locked ultrafast laser based on a femtosecond-laser-inscribed in-fiber Brewster device. *Opt. Lett.* **2019**, *44*, 5177–5180. [CrossRef] [PubMed]
6. Hu, P.; Mao, J.J.; Zhou, X.; Feng, T.L.; Nie, H.K.; Wang, R.H.; Zhang, B.T.; Li, T.; He, J.L.; Yang, K.J. Multiple soliton mode-locking operations of a Holmium-doped fiber laser based on nonlinear polarization rotation. *Opt. Laser Technol.* **2023**, *161*, 109218. [CrossRef]
7. Matsas, V.; Newson, T.; Richardson, D.; Payne, D.N. Self-starting, passively mode-locked fibre ring soliton laser exploiting non-linear polarisation rotation. *Electron. Lett.* **1992**, *28*, 1391–1393. [CrossRef]
8. Wu, X.; Tang, D.Y.; Zhang, H.; Zhao, L.M. Dissipative soliton resonance in an all-normal-dispersion erbium-doped fiber laser. *Opt. Express* **2009**, *17*, 5580–5584. [CrossRef] [PubMed]
9. Li, Y.Y.; Jiang, M.; Hou, L.; Tao, J.N.; Song, P.Y.; Lu, B.L.; Bai, J.T. Wavelength-tunable dissipative soliton from Yb-doped fiber laser with nonlinear amplifying loop mirror. *Chin. Opt. Lett.* **2023**, *21*, 061402. [CrossRef]
10. Li, H.J.; Li, X.L.; Zhang, S.M.; Liu, J.M.; Yan, D.; Wang, C.R.; Li, J.Y. Vector Staircase Noise-Like Pulses in an Er/Yb-Codoped Fiber Laser. *J. Light. Technol.* **2022**, *40*, 4391–4396. [CrossRef]
11. Tao, J.N.; Song, P.Y.; Lv, C.Y.; Hou, L.; Lu, B.L.; Bai, J.T. Generation of widely tunable single- and dual-wavelength in a figure-eight mode-locked fiber laser. *Opt. Laser Technol.* **2023**, *160*, 109107. [CrossRef]
12. Tao, J.N.; Song, Y.Q.; Li, Y.Y.; Jia, X.Z.; Hou, L.; Lu, B.L.; Bai, J.T. Pulse type switchable, spectral bandwidth dynamically adjustable all-fiber laser mode-locked by NALM. *Opt. Laser Technol.* **2023**, *157*, 108682. [CrossRef]
13. Jiang, H.; Li, H.; Hu, F.; Ren, X.; Li, C.; Xu, S. Mode-locked Tm fiber laser with a tapered GIMF SA based on nonlinear multimode interference effect. *IEEE Photonics Technol. Lett.* **2020**, *32*, 503–506. [CrossRef]
14. Zhang, B.; Ma, S.; Lu, S.; He, Q.; Guo, J.; Jiao, Z.; Wang, B. All-fiber mode-locked ytterbium-doped fiber laser with a saturable absorber based on the nonlinear Kerr beam cleanup effect. *Opt. Lett.* **2020**, *45*, 6050–6053. [CrossRef] [PubMed]
15. Dong, Z.; Lin, J.; Li, H.; Zhang, Y.; Gu, C.; Yao, P.; Xu, L. Er-doped mode-locked fiber lasers based on nonlinear polarization rotation and nonlinear multimode interference. *Opt. Laser Technol.* **2020**, *130*, 106337. [CrossRef]
16. Fermann, M.; Sugden, K.; Bennion, I. Generation of 10 nJ picosecond pulses from a modelocked fibre laser. *Electron. Lett.* **1995**, *31*, 194–195. [CrossRef]
17. Ilday, F.; Buckley, J.; Kuznetsova, L.; Wise, F. Generation of 36-femtosecond pulses from a ytterbium fiber laser. *Opt. Express* **2003**, *11*, 3550–3554. [CrossRef]
18. Ahmad, H.; Azmy, N.F.; Norisham, N.F.; Reduan, S.A.; Zulkifli, M.Z. Thulium-doped fluoride mode-locked fiber laser based on nonlinear polarization rotation. *Opt. Quant. Electron.* **2022**, *54*, 80. [CrossRef]
19. Mou, C.B.; Wang, H.; Bale, B.G.; Zhou, K.M.; Zhang, L.; Bennion, I. All-fiber passively mode-locked femtosecond laser using a 45°-tilted fiber grating polarization element. *Opt. Express* **2010**, *18*, 18906–18911. [CrossRef]
20. Du, Y.Q.; Shu, X.W.; Xu, Z.W. All-fiber passively mode-locked laser based on a chiral fiber grating. *Opt. Lett.* **2016**, *41*, 360–363. [CrossRef]
21. Alamgir, I.; Rochette, M. Thulium-doped fiber laser mode-locked by nonlinear polarization rotation in a chalcogenide tapered fiber. *Opt. Express* **2022**, *30*, 14300–14310. [CrossRef]
22. Erdogan, T. Fiber grating spectra. *J. Light. Technol.* **1997**, *15*, 1277–1294. [CrossRef]
23. Hill, K.O.; Meltz, G. Fiber Bragg grating technology fundamentals and overview. *J. Light. Technol.* **1997**, *15*, 1263–1276. [CrossRef]

24. Bhatia, V.; Campbell, D.K.; Sherr, D.; D'Alberto, T.; Zabaronick, N.; Ten Eyck, G.A.; Murphy, K.A.; Claus, R.O. Temperature-insensitive and strain-insensitive long-period grating sensors for smart structures. *Opt. Eng.* **1997**, *36*, 1872–1876. [CrossRef]

25. Costantini, D.; Limberger, H.; Salathe, R.; Muller, C.; Vasiliev, S. Tunable loss filter based on metal coated long period grating. In Proceedings of the 24th European Conference on Optical Communication, ECOC'98 (IEEE Cat. No. 98TH8398), Madrid, Spain, 20–24 September 1998; pp. 391–392.

26. Liu, Y.; Zhang, L.; Williams, J.; Bennion, I. Bend sensing by measuring the resonance splitting of long-period fiber gratings. *Opt. Commun.* **2001**, *193*, 69–72. [CrossRef]

27. Bilodeau, F.; Johnson, D.; Theriault, S.; Malo, B.; Albert, J.; Hill, K. An all-fiber dense wavelength-division multiplexer/demultiplexer using photoimprinted Bragg gratings. *IEEE Photonic Technol. Lett.* **1995**, *7*, 388–390. [CrossRef] [PubMed]

28. Shen, F.; Wang, C.; Sun, Z.; Zhou, K.; Zhang, L.; Shu, X. Small-period long-period fiber grating with improved refractive index sensitivity and dual-parameter sensing ability. *Opt. Lett.* **2017**, *42*, 199–202. [CrossRef]

29. Kanagaraj, N.; Theodosiou, A.; Aubrecht, J.; Peterka, P.; Kamradek, M.; Kalli, K.; Kasik, I.; Honzatko, P. All fiber mode-locked thulium-doped fiber laser using a novel femtosecond-laser-inscribed 45°-plane-by-plane-tilted fiber grating. *Laser Phys. Lett.* **2019**, *16*, 095104. [CrossRef]

30. Wang, T.; Yan, Z.; Mou, C.; Liu, Z.; Liu, Y.; Zhou, K.; Zhang, L. Narrow bandwidth passively mode locked picosecond Erbium doped fiber laser using a 45 degrees tilted fiber grating device. *Opt. Express* **2017**, *25*, 16708–16714. [CrossRef] [PubMed]

31. Shen, F.; Shu, X.; Zhou, K.; Jiang, H.; Xia, H.; Xie, K.; Zhang, L. Compact vector twist sensor using a small period long period fiber grating inscribed with femtosecond laser. *Chin. Opt. Lett.* **2021**, *19*, 090601. [CrossRef]

32. Zhao, R.; Liu, H.; Shu, X. Femtosecond laser-inscribed off-axis high-order mode long-period grating for independent sensing of curvature and temperature. *Opt. Express* **2022**, *30*, 37697–37710. [CrossRef] [PubMed]